Solid State Ionics 39 (1990) 81–89
North-Holland

VIBRATIONAL THRESHOLDS IN COVALENT NETWORKS

P. BOOLCHAND, R.N. ENZWEILER [1]
Department of Electrical and Computer Engineering and Department of Physics, University of Cincinnati, Cincinnati, OH 45221, USA

R.L. CAPPELLETTI
Department of Physics and Astronomy and Condensed Matter and Surface Sciences Program, Ohio University, Athens, OH 45701, USA

W.A. KAMITAKAHARA
Ames Laboratory and Department of Physics, Iowa State University, Ames, IO 50011, USA

Y. CAI and M.F. THORPE
Physics and Astronomy Department and Center for Fundamental Materials Research, Michigan State University, East Lansing, MI 48824, USA

Received January 1990

Vibrational thresholds in covalent networks predicted theoretically have been observed in chalcogenide glasses. The experiments have included Mössbauer–Debye–Waller factors, inelastic neutron scattering, Raman scattering and ultrasonic elastic moduli.

1. Introduction

Vibrational thresholds in covalent networks represent a recent subject in condensed matter science where theory and experiment have rapidly converged to capture the essence of basic ideas. The tools have included Lagrangian mechanics and vibrational spectroscopy. These thresholds are largely determined by a single structure variable-average coordination number $\langle m \rangle$. It also appears that these thresholds are related to more distant atomic structure correlations of a glass network, (medium range order) albeit in a more subtle manner.

Diffuse scattering experiments on glasses performed over the past eighty years have shown that short-range order in glasses and corresponding crystalline materials are rather similar [1] (Ioffe–Regel rule). This led Phillips [2] to introduce the notion that bond-stretching (α) and bond-bending (β) forces in covalent glasses may be visualized to act as mechanical constraints (N_c). Phillips proceeded to suggest that when the number of atomic degrees of freedom (N_d) exhaust the number of constraints per atom (N_c), an optimum condition for determinative but unstressed mechanical stability of a covalent network must prevail.

$$N_c = N_d \,. \tag{1}$$

Since the number of α- and β-constraints increases with m, in 3-dimensions, eq. (1) implies a privileged average coordination number $\langle m \rangle = 2.40$.

Thorpe [3] recognized that the glass condition (1) can be cast in terms of a percolation problem in which the quantity of interest is "rigidity", i.e., resistance to deformation of a covalent network. He showed that for a 3-dimensional network that is undercoordinated i.e. $\langle m \rangle < 2.4$, a finite number of "zero-frequency" or "floppy modes" must occur. On the other hand, when a network becomes over-coordinated

[1] Present address: Department of Physics, State University of New York College at Cortland, Cortland, NY, USA.

0167-2738/90/$ 03.50

($\langle m \rangle > 2.4$), rigid modes are pervasive. Viewed in this manner, the glass condition becomes a floppy to rigid vibrational mode transition with a very specific prediction, viz, the number of floppy modes approaches zero as $\langle m \rangle$ approaches 2.40 from below. One cannot overemphasize the importance of these simple but profound theoretical ideas, since in nature some of the best inorganic glasses (As_2S_3, SiO_2) completely satisfy the glass condition (1).

It is of interest to inquire if vibrational thresholds have been observed in real glasses and in particular how do experimental observations compare to the theoretical predictions. It is the purpose of this article to address the experimental status in this regard.

2. Inorganic network glasses

Binary glasses A_xB_{1-x}, where A = pnictide (P, As and Sb) or tathogen (Si, Ge and Sn) and B = chalcogen (S, Se and Te) are preferred over the oxide glasses for the present investigation since these can be prepared over a broad range of stoichiometries. Since chalcogens, pnictides, and tathogens usually bond with a coordination number of 2, 3 and 4, the average coordination number ($\langle m \rangle$ of a glass is easily deduced once its composition is known. Thus in the case of binary Ge_xSe_{1-x} glasses, since $\langle m \rangle = 2(1+x)$, $\langle m \rangle$ can be continuously tuned in the range $2 < \langle m \rangle < 2.67$, with $\langle m \rangle = 2.4$ at $x = 0.20$, the mechanical or vibrational threshold. Furthermore, for the present investigations, chalcogenide glasses of tathogens (such as Ge_xSe_{1-x}) are preferred over their pnictide counterparts (As_xSe_{1-x}), because the former glasses comprise of an overconstrained ($\langle m \rangle = 2.67$) tetrahedral unit $Ge(Se_{1/2})_4$ while the latter glasses, comprise of an optimally constrained ($\langle m \rangle = 2.40$) pyramidal unit $As(Se_{1/2})_3$. This has the important consequence [4] that in tathogen based glasses, the mechanical (x_m) and chemical (x_c) threshold occur at different stoichiometries ($x_m = 0.20$, $x_c = 0.33$) and are thus easily separated. In pnictide glasses on the other hand, the chemical threshold at $x_c = 0.40$ corresponds to the crystalline compound As_2Se_3, and it coincides with the mechanical one ($x_m = 0.40$). The latter makes it difficult to separate the two types of physical effects. For this reason we have chosen to examine binary Ge_xSe_{1-x} glasses in vibrational spectroscopy experiments.

3. Experimental probes

Perhaps some of the most direct probes of floppy modes in glasses can be grouped under the term vibrational spectroscopy and include inelastic neutron scattering [5], Mössbauer vibrational spectroscopy [6] and Raman scattering [7]. Other types of experiments, more indirect in nature, have also shed light on the basic problem, by addressing mechanical properties, physical and chemical aspects of glass structure near the ridigity threshold. These experiments include bulk elastic constants [8,9] and acoustic attenuation [10] both studied by ultrasonics, network packing as established by molar volume measurements [11], glass crystallization temperatures measured by scanning calorimetry [12], semiconducting to metal transition pressures established by electrical conductivity measurements [13], and electric field gradient distributions [14] in Mössbauer spectroscopy experiments. Consequences of some of these investigations have been discussed in previous articles [15]. Here we will focus on some recent results of inelastic neutron scattering and Mössbauer vibrational spectroscopy on Ge_xSe_{1-x} glasses.

4. Inelastic neutron scattering

The left panel of fig. 1 displays neutron density of vibrational states (DOVS) at selective compositions in binary Ge_xSe_{1-x} glasses taken from the work of Kamitakahara et al. [5]. Perhaps the most striking feature of these data is the appearance of a low energy vibrational band centered at about 4 meV (or 32 cm^{-1}), the integrated strength of which in the 0–8 meV (shaded) region represents 1/3rd of the total VDOS in g-Se. This constitutes good evidence that the band in question represents the "floppy modes" because the fraction "f" of zero-frequency modes in a network of average coordination number $\langle m \rangle$ is given [16] by

$$f = 2 - 5/6 \langle m \rangle , \qquad (2)$$

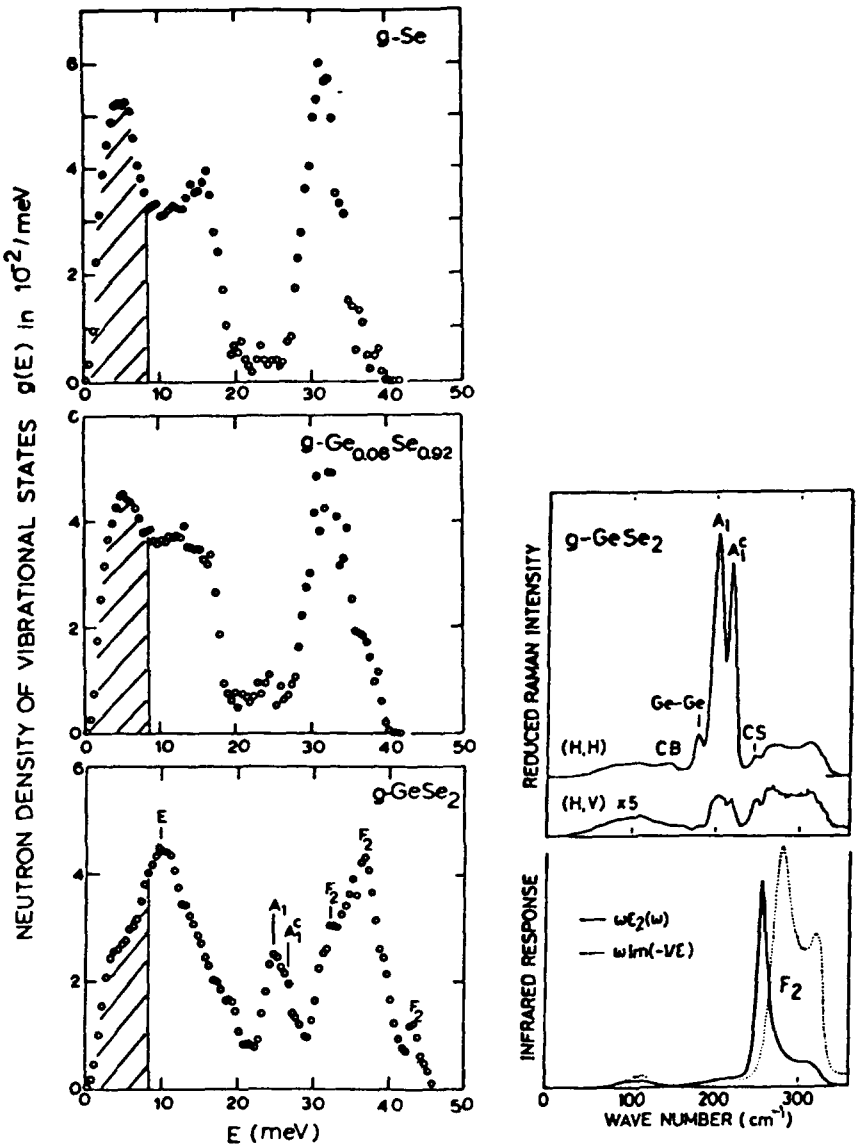

Fig. 1. Neutron density of vibrational states (left panel) in Ge_xSe_{1-x} glasses illustrating the floppy modes (shaded region) strength qualitatively reducing with Ge alloying. These results are taken from the work of Kamitakahara et al. (ref. [5]). The right panel shows infrared and Raman spectra of g–$GeSe_2$ taken from the work of Murase and Fukanaga (ref. [7]).

and it yields $f = 1/3$ at $\langle m \rangle = 2$ appropriate for g–Se. Furthermore, Ge alloying in a Se glass leads to a rapid decline in the fraction "f" of floppy modes, as seen qualitatively from the VDOS of fig. 1. In under-coordinated glasses the zero-frequency modes are believed to be shifted up to a finite frequency because weaker dihedral-angle and Van der Waals forces must inevitably supplement the covalent α and β forces to insure mechanical stability of networks. Recent calculations of Cai and Thorpe [17] show that the effect of these weaker forces is to smear the kink at $\langle m \rangle = 2.4$. A point of disagreement between theory and experiment, however, is the continued presence of low-frequency modes at Ge concentra-

tions $x \gtrsim 0.20$. Regardless of how one wishes to interpret the low-frequency excitations in Ge_xSe_{1-x} glasses at $x \gtrsim 0.20$, the presence of such excitations in the DOVS may be indicative that simple random networks as used in the present theoretical calculations may not be adequate to describe real glasses.

The neutron DOVS in $GeSe_2$ glass display several sharp modes at $E > 10$ meV, that are easily identified as normal modes (A_1, E, F_2) of a $Ge(Se_{1/2})_4$ tetrahedral unit – the building block of the glass network. These mode identifications are greatly facilitated by a comparison of the neutron to the Raman- and IR-DOVS shown in the right panel of fig. 1. Furthermore, the companion A_1 mode (A_1^c) at 26.8 meV or 216 cm^{-1} is also observed in the neutron-spectra as it is in the Raman-spectra. An extensive discussion of threshold behavior in Raman and IR mode frequencies at the rigidity threshold has been given by Murase and Fukunaga [18] and independently by Phillips [19].

5. Mössbauer spectroscopy

Applications of Mössbauer spectroscopy as a probe of glass molecular structure has been discussed in several reviews by Boolchand [20]. The experiments to date have focussed on decoding hyperfine structure to establish the nature of chemical sites of isovalent additives such as ^{119}Sn for Ge or ^{125}Te and $^{129}Te^m$ for Se in a chalcogenide glass such as Ge_xSe_{1-x}. Thus such experiments have shown that ^{119}Sn spectra of bulk $(Ge_{0.99}Sn_{0.01})_xSe_{1-x}$ glasses display a narrow single line possessing an isomer-shift characteristic of a tetrahedral $Sn(Se_{1/2})_4$ site (site A) in the composition range $0 < x < 0.30$, but in fact two distinct sites (A, B) near and at the stoichio-

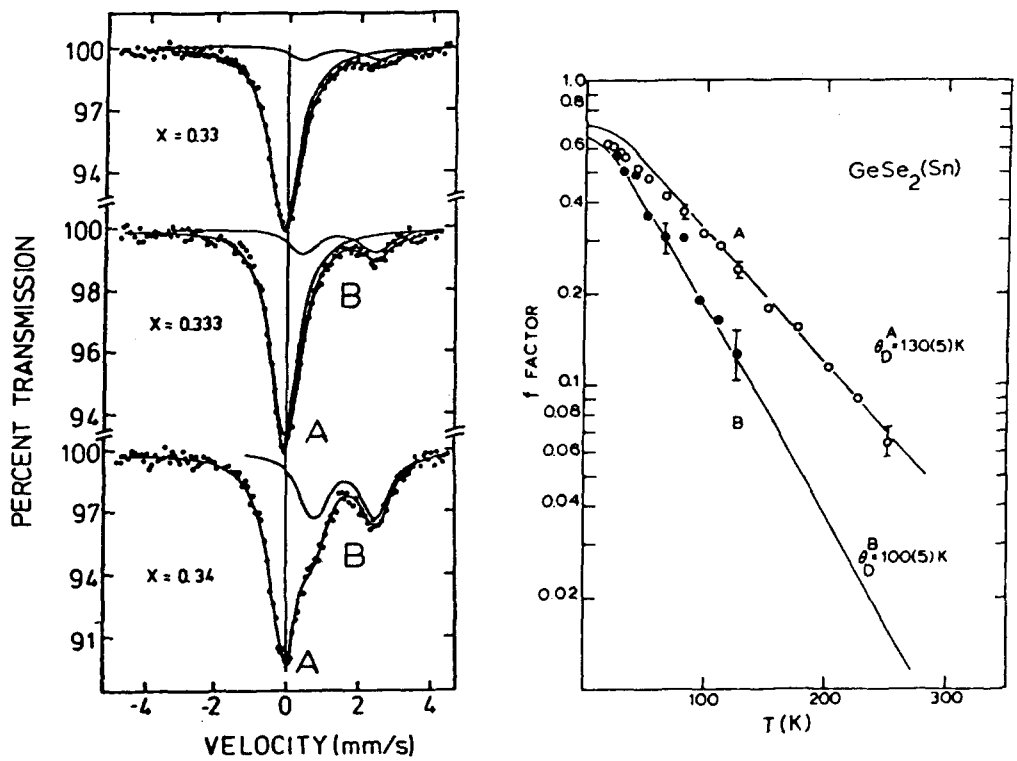

Fig. 2. (a) ^{119}Sn Mössbauer spectra of $(Ge_{0.99}Sn_{0.01})_xSe_{1-x}$ glasses showing two sites (A, B) near the stoichiometric composition $x = 0.333$. These spectra are taken from the work of Boolchand et al. [14]; (b) T-dependence of the integrated intensity of site A (singlet) and site B (doublet) revealing the widely different vibrational (Debye) temperatures θ_D.

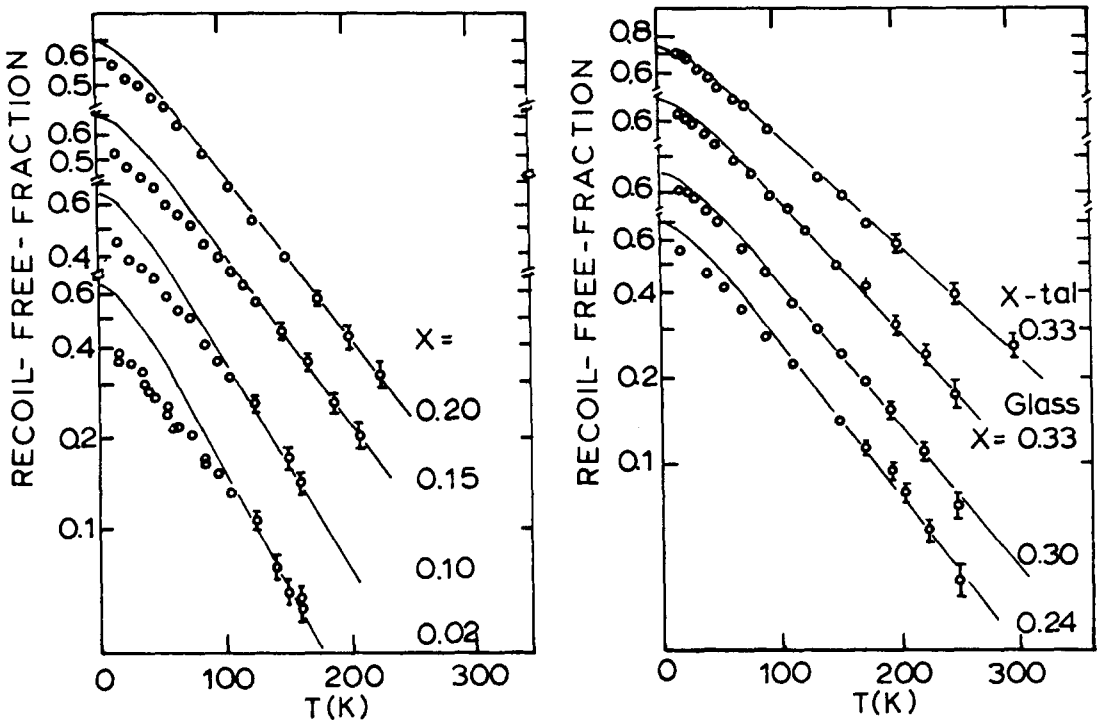

Fig. 3. Site A T-dependence of the Mössbauer–Debye–Waller factor $f(t)$ in $(Ge_{0.99}Sn_{0.01})_xSe_{1-x}$ glasses at indicated cation concentrations x. In C–$GeSe_2$, note that $f(t)$ is well fit by one Debye temperature, while in glasses a softening of $f(T)$ is observed at low-T on account of the floppy modes.

metric composition $x=1/3$, i.e. $GeSe_2$ glass (fig. 2). The second site, site B, characterized by a doublet, is ascribed to a non-tetrahedral Sn site, with the site intensity ratio $I_B/(I_B+I_A)=0.16(1)$, and provides evidence [21] of molecular phase separation in the stoichiometric glass.

Because of the zero-phonon nature of Mössbauer absorption, as in X-ray Bragg scattering, the integrated area under a resonance varies with temperature determined by the Debye–Waller factor or f-factor given by eq. (3)

$$f=e^{-\langle(\boldsymbol{k}.\boldsymbol{u})^2\rangle} \tag{3}$$

where $\boldsymbol{k}$ is the γ-ray wave vector and $\boldsymbol{u}$ displacement vector of the Mössbauer active nucleus. At low T, the mean square displacement

$$\langle u^2\rangle T\to 0\simeq \frac{3h}{2M\omega} \tag{4}$$

while at high T, it equals

$$\langle u^2\rangle T>\theta=\frac{3k_BT}{M\omega^2}. \tag{5}$$

This leads to a characteristic T-dependence [22] of the mean square displacement $(-\ln f)$ which saturates at low T, but becomes linear at high T, as shown in fig. 2 for sites A and B observed in $GeSe_2$ glass, for example. From eqs. (5) and (4) it follows that the slope $d(-\ln f)/dT$ provides a measure of the second-inverse moment while the $T\to 0$ f-factor (f_0), a measure of the first-inverse moment of the DOVS. Specifically one can show that

$$\left\langle\frac{1}{\omega^2}\right\rangle=\frac{\hbar^2Mc^2}{E_\gamma^2}\frac{1}{k_B}\frac{d}{dT}(-\ln f), \tag{6}$$

$$\left\langle\frac{1}{\omega}\right\rangle=\frac{\hbar Mc^2}{E_\gamma^2}(-\ln f_0), \tag{7}$$

where E_γ and M represent the Mössbauer γ-ray energy of 23.8 keV and atomic mass of ^{119}Sn.

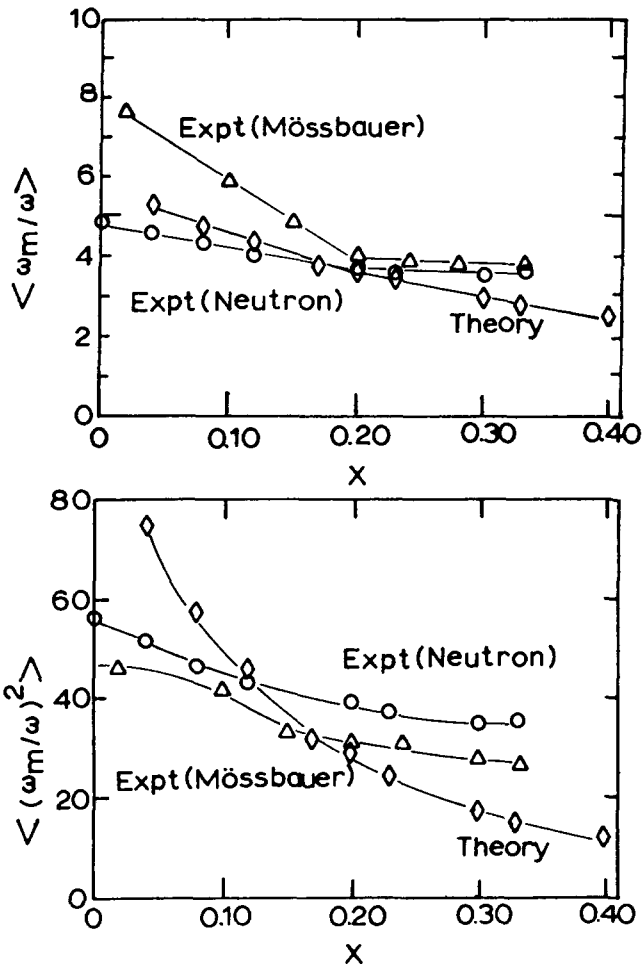

Fig. 4. First inverse $\langle \omega_m/\omega \rangle$ (top pannel) and second inverse $\langle (\omega_m/\omega)^2 \rangle$ (bottom panel) moments of the density of vibrational states deduced from inelastic neutron scattering (O), Mössbauer–Debye–Waller factors (△) and bond-depleted diamond lattice calculations (◇) as a function of Ge concentration x. Note that $\langle \omega_m\omega \rangle$ displays clear evidence of a break in slope near $x=0.20$ corresponding to the rigidity threshold.

The f-factor results for the two sites (A, B) in g-$GeSe_2$ (fig. 2) carry an important message. One would be hard pressed to explain a significant reduction in the B-site f-factor in relation to the A-site one, if both these sites were to be formed in a continuous random network of $Ge(Se_{1/2})_4$ units. Site A represents the chemically ordered site while site B the chemically disordered defect site formed when a Ge–Se bond is replaced by a Ge–Ge bond. On the other hand, the observed result is the expected result if A and B sites represent Sn replacing Ge in two distinct clusters – a tetrahedral A cluster and a non-tetrahedral B cluster as suggested elsewhere [23].

Site A T-dependence of f-factors in $(Ge_{0.99}Sn_{0.01})_xSe_{1-x}$ glasses and in crystalline $Ge_{0.99}Sn_{0.01}Se_2$ appear in fig. 3. The continuous lines drawn through these plots are predictions based on a Debye-like DOVS and are merely meant to set the ordinate scale by matching the high-T linear slope $d(-\ln f)/dT$ which uniquely fixes a Debye-temperature θ_D. Perhaps the most striking feature of the results is the qualitative softening of the f-factor or enhanced mean-square-displacement encountered in the undercoordinated glasses, i.e. at $x \lesssim 0.20$.

We can begin to see that the enhanced mean-square-displacement of a $Sn(Se_{1/2})_4$ unit in underconstrained glasses derives from the presence of the floppy modes in the DOVS. The large density of states under these modes enhances $\langle u^2 \rangle$ as $T \to 0$ and causes the f-factor to qualitatively soften. To make a more quantitative comparison between the neutron and Mössbauer results, we have deduced the first-inverse and second-inverse moments as a function of glass composition from both type of experiments and the results are summarized in fig. 4. Before discussing the consequences of these experimental results, it would be appropriate to comment on the theory which is used to compare these results. Results of ultrasonic elastic moduli on these glasses are also available and we comment on these as well.

6. Ultrasonic elastic moduli

Recent room temperature measurements of elastic moduli in Ge_xSe_{1-x} glasses by the pulse-echo ultrasonic technique in the 20 MHz range provide a means of directly probe the macroscopic mechanical properties of these glasses [8]. Liquid helium measurements of elastic moduli in these glasses reported by Duquesne and Bellessa [9] also reveal results that are parallel to the room temperature ones shown here in fig. 5. The prediction of a kink in the longitudinal and transverse elastic moduli at $\langle m \rangle = 2.4$ by He and Thorpe [24] was not borne out in both measurements. More recently Cai and Thorpe [17] have

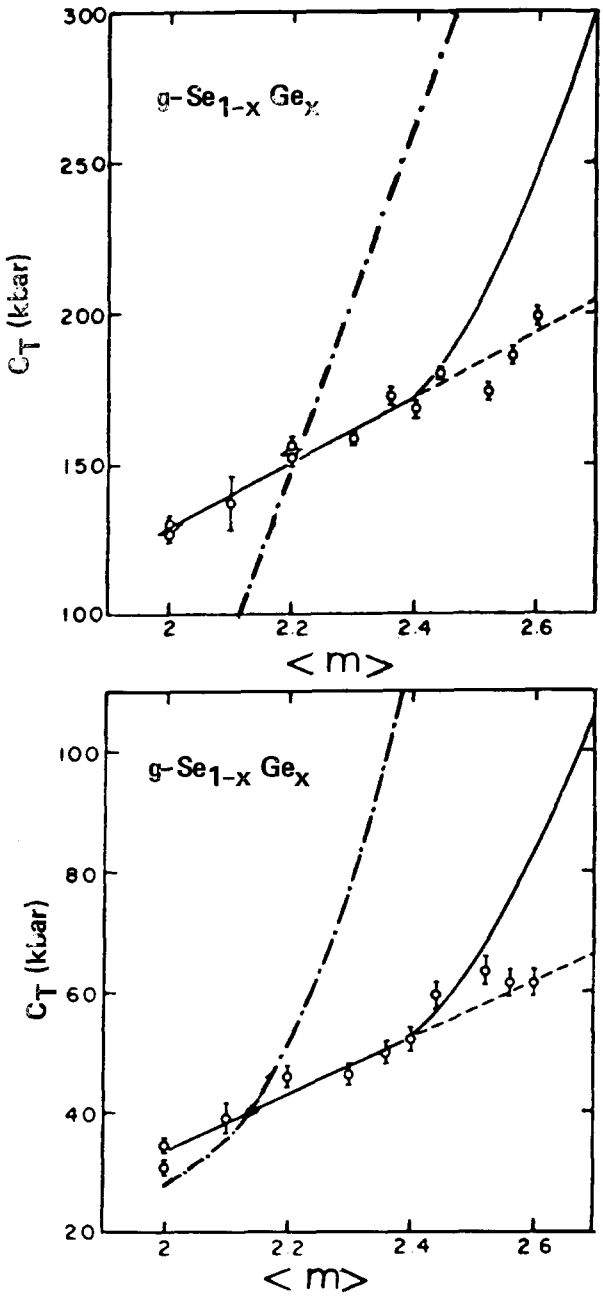

Fig. 5. Longitudinal C_L (top panel) and Transverse C_T (bottom panel) elastic moduli of Ge_xSe_{1-x} glasses plotted as a function of $\langle m\rangle = 2(1+x)$ showing no threshold behavior at $\langle m\rangle = 2.4$. The solid line is the prediction of the bond-depleted diamond lattice including α and β forces only, but modified empirically to include a background elastic property (ref. [24]). The long-dash line is the prediction of the same model now including dihedral angle and interchain forces (ref. [17]). The experiments are due to ref. [8].

found that including dihedral angle and interchain forces smears out the kink, in agreement with these elastic constant results, but their detailed predictions (long-dash lines in fig. 5) for the elastic constants remain in significant disagreement with the experiments. The coefficient of the ω^2 term in the DOVS calculated from these ultrasonic data is in good agreement with the neutron measurements at low frequencies, and this shows that the lowest frequency behavior is dominated by acoustic modes, not floppy ones. This fact allows us to understand the discrepancy between the experimental and theoretical results for the second inverse moment displayed in fig. 4. Since the Cai and Thorpe theory gives softer behavior than experiment for the elastic moduli below $\langle m\rangle = 2.2$ and harder behavior than experiment above that value one can see that the second inverse moment, which goes like an appropriate average of the elastic moduli to the $-3/2$ power, will disagree with experiment in the way shown. The fact that the crossover occurs with the neutron data at $x=0.1$ ($\langle m\rangle = 2.2$) is simply a reflection of the agreement between the neutron and ultrasonic results. We believe that these subtle discrepancies between theory and experiment hold a clue for the structure of these glasses as will be discussed later.

7. DOVS calculations in a bond-depleted-diamond lattice

Continuous random networks of average coordination number in the range $2.08 < \langle m\rangle < 4$ can be constructed by randomly cutting bonds of a cubic diamond lattice following a procedure described by He and Thorpe [24]. Next one introduces a potential

$$V = \frac{\alpha}{2}\sum_{ij}[(\boldsymbol{u}_i - \boldsymbol{u}_j)\cdot\hat{r}_{ij}]^2 + \frac{\beta}{2}\sum_{ijk} l_{ij}l_{jk}[\Delta\theta_{ijk}]^2, \qquad (8)$$

to include bond-stretching (α) and bond-bending (β) covalent forces and examine eigenmodes of the system when atoms are given a small virtual displacement from their quasi-equilibrium position. Thorpe and Cai [16] have investigated the VDOS of such networks as a function of $\langle m\rangle$ and have obtained resonable accord with the neutron-VDOS by adjusting the coefficients α and β in the potential given by eq. (8). This surprising observation un-

derscores the fact that network connectivity or average coordination number is the singly most important structure parameter that determines the broad features of the VDOS. The network morphology or medium range order is much less sensitive to the VDOS. From the calculated VDOS, these workers have projected the first- and second-inverse moments. The effect of including weaker dihedral angle and van der Waals forces in the interatomic potential has also been examined recently [17]. These authors find that the presence of weaker forces apparently smears the kink at the rigidity threshold, although the qualitative features of the VDOS remain largely unchanged. The first-inverse and second-inverse moment from these theoretical calculations are also plotted in fig. 4, to afford a comparison with the experimental results.

8. Discussion

The most striking observation to emerge from the plots of fig. 4, is the presence of a threshold behavior in the first-inverse moment (top panel) of the VDOS. The theory as well as both the experiments described indicate a mild but unmistakable break in slope that is localized at or near $x=0.20$. It is identified with the percolation of rigidity. One can physically trace this effect to the qualitative presence of the low-frequency floppy modes at $x<0.20$, that weigh heavily in the first-inverse moment. Evidently, the discrepancy between the structure of the model and that of real glasses plays little role in determining the behaviour of the floppy modes. It is remarkable and satisfying that this simple model can account for the principal features in the vibrational thresholds of real glasses.

The situation for the second inverse moment (bottom pannel of fig. 4) is more speculative at this stage. This moment weighs heavily the lowest frequency excitations which include besides floppy modes, acoustic modes, inter-layer modes, cluster-surface or edge modes, etc. The presence of these low frequency modes apparently smears the threshold behavior at $x=0.20$ as can be seen from the experimental results and theoretical calculations shown in fig. 4 (bottom panel). Furthermore, we find that the comparison between the present theory and experiments for the second-moment is not as good as noted above for the first inverse moment. Unlike the floppy modes, whose strength depends exclusively on elements of short range order ($\langle m \rangle$), the other lowest frequency excitations indicated above can be expected to be sensitive to the more distant atomic structure correlations (medium range order) in a real glass. The discrepancy between the experiment and theory in the second inverse moment (bottom panel of fig. 4) arises, as discussed above, from the same feature of the theory which causes disagreement in the elastic moduli. We suggest, therefore, that the second inverse moment and elastic moduli are more sensitive to intermediate range structural order in these glasses which, in turn, as implied by the Mössbauer hyperfine structure results is connected to the presence of molecular phase separation as discussed elsewhere [14,15]. Clearly, such structure cannot be represented by the bond-depleted diamond lattice. This point of view is supported by the other notable discrepancy between theory and experiment, namely the persistence of a small floppy shoulder beyond $\langle m \rangle = 2.4$.

In summary, the present work demonstrates that vibrational thresholds due to floppy modes are clearly observed in the first inverse moment of the DOVS as revealed in inelastic neutron scattering and Mössbauer–Debye–Waller factor experiments, in harmony with the predictions of the depleted diamond lattice calculations of Cai and Thorpe.

Acknowledgement

This work was supported in part by the U.S. National Science Foundation under grant DMR-85-21005 and DMR-89-02836 and the Office of Naval Research under contract number N00014-80-C-0610.

References

[1] A.F. Ioffe and A.R. Regel, Proc. Semiconductors. 4 (1960) 237.
[2] J.C. Phillips, J. Non-Cryst. Solids 43 (1981) 37.
[3] M.F. Thorpe, J. Non-Cryst. Solids 57 (1983) 355.
[4] P. Boolchand, Phys. Rev. Letters 57 (1986) 3233.

[5] W.A. Kamitakahara, P. Boolchand and R.L. Cappelletti, 12th Internat. Conf. IR and MM Waves (Dec. 1987, Florida).
[6] P. Boolchand, R.N. Enzweiler, R.L. Cappelletti, W.A. Kamitakahara, Y. Cai and M.F. Thorpe, unpublished.
[7] K. Murase and T. Fukunaga, in: Defects in glasses, Mat. Res. Soc. Symp. Proc. 61 (1986) 101.
[8] S.S. Yun, Hui Li, R.L. Cappelletti, R.N. Enzweiler and P. Boolchand, Phys. Rev. B 39 (1989) 8702;
also see B.L. Halfpap and S.M. Lindsay, Phys. Rev. Letters 5 (1986) 847;
Also see I. Ito, S. Kashida and K. Murase, Solid State Commun. 65 (1988) 449.
[9] J.Y. Duquesne and G. Bellessa, Europhys. Letters, to be published; J. Phys. (Paris) Colloq. 46 (1985) C10445.
[10] K.S. Gilroy and W.A. Phillips, Philos. Mag. B 47 (1983) 655.
[11] A. Feltz, H. Aust and A. Bleyer, J. Non-Cryst. Solids 55 (1983) 179.
[12] B. Norban, D. Pershing, R.N. Enzweiler, P. Boolchand, J.E. Griffiths and J.C. Phillips, Phys. Rev. B 36 (1987) 8109.
[13] S. Asokan, M.V.N. Prasad, G. Parthasarathy, E.S.R. Gopal, Phys. Rev. Letters 62 (1989) 808.
[14] W. Bresser, P. Boolchand and P. Suranyi, Phys. Rev. Letters 56 (1986) 2493.
[15] P. Boolchand, in: Metallic and semiconducting glasses I, Trans. Tech. Publ., Key Engineering Materials 13–15 (1987) 131.
[16] M.F. Thorpe and Y. Cai, in: Proc. Internat. School on Condensed Matter Physics, (Bulgaria 1988).
[17] Y. Cai and M.F. Thorpe, unpublished.
[18] K. Murase and T. Fukunaga, in: Proc. 17th Internat. Conf. Physics of Semiconductors, ed. by J.D. Chadi and W.A. Harrison (Springer, New York, 1985) p. 943.
[19] J.C. Phillips, Phys. Rev. B 31 (1985) 8157.
[20] P. Boolchand, in: Physical properties of amorphous materials, eds. D. Adler, B.B. Schwartz and M.C. Steele (Plenum, New York, 1985) p. 221.
[21] P. Boolchand, J. Grothaus, W.J. Bresser and P. Suranyi, Phys. Rev. B25 (1982) 2975.
[22] N.N. Greenwood and T.C. Gibb, Mössbauer spectroscopy (Chapman and Hall, (London, 1971) p. 11.
[23] P. Boolchand, J. Grothus and J.C. Phillips, Solid State Commun. 45 (1983) 183.
[24] H. He and M.F. Thorpe, Phys. Rev. Letters 54 (1985) 2107.